Nanoliquids flow due to a stretching sheet and the behavior of heat and mass transfer: an analysis with an OHAM Solution

MN Raja Shekar
Department of Mathematics,
JNTUH College of Engineering Jagitial- 505501, Telangana, India

Abstract : This paper analyzes Nanoliquids flow over a stretching sheet and the characteristics of heat and mass transfer with uniform heat generation.Cu-water and Ag-water nanoliquids are considered in the study. To obtain a system of the non-linear ordinary differential equation similarity variables have been applied and an optimal homotopy asymptotic method (OHAM) have been used to work out these equations. Various parametric influences on the velocity, temperature, and mass transfer have been shown by means of tables and graphs and the result we found is in an excellent agreement with the previous results in the literature. It was displayed that the Ag-water nanoliquid exhibits higher thermal conductivity compared to Cu-water nanoliquid. In addition, the presence of a uniform heat source has a reducing effect on the concentration profile and increasing effect on the temperature.

IndexTerms **- Nanoliquid flow, OHAM, Stretching sheet, Soret number,Schmidt number,heat generation**

I. INTRODUCTION

A flow on a stretching surface has fascinated the concentration of many researchers over the past few decades because of its application in the field of engineering. Some of its application are like melt-spinning, etc. The first person who studied about a two-dimensional steady Newtonian fluid passion, in extrusion processes, wire drawing, the manufacture of plastic, the performance of lubricants by a stretching elastic sheet with a linearly varying velocity a certain distance from a fixed point moving in its plane was Crane [1]. Later on, this work has been extended by several authors to discover various aspects of the flow and a fluid heat transfer of infinite extent neighboring a stretching sheet. The following are amongst them. Awaludin et al. [2], Noor and Hashim [3], Reda G. Abdel-Rahman [4], Bhattacharyya et al. [5], Reza et al. [6], Ullah et al. [7], Ahmad and Ishak [8], Shah et al. [9]. Kameswaran et al. [10] investigated the convective transfer of heat and mass in a Nanofluid flow over a sheet stretched subject to viscous dissipation, hydromagnetic, chemical reaction and Soret effects. They obtained that the Ag-Water Nanofluid exhibits lower rates of wall heat and mass transfer comparing withCu-water Nanofluid.

Raju et al. [11] presented his study on MHD Casson fluid and the behavior of heat and mass transport over an exponentially stretching permeable surface in the incidence of parameters like viscous dissipation, thermal radiation, chemical reaction, and magnetic field. Also, the MHD flow of a Jeffery fluid through a porous media over a stretching sheet under chemical reaction effect with heat generation has been studied by Jena et al. [12]. Their result has shown that the distribution of a temperature in the flow domain was enhanced by the porous matrix and magnetic field. Velocity slip parameter and heat source influences on MHD flow of a Jeffery fluid on a stretching surface were analyzed by Gizachew and Shankar [13]. Furthermore, Gaffar et al. [14] examined a steady boundary layer flow of an incompressible non-Newtonian Jeffery's fluid past a semi-infinite non-linear vertical plate. Ali et al. [15]studied a viscous MHD flow of a fluid problem on a porous non-linear shrinking sheet. In their study, they have found that dual solutions exist only for positive values of the controlling parameter. The transfer of heat on a fluid and an MHD Boundary layer flow with variable viscosity in a porous medium towards a stretching sheet with an influence of viscous dissipation in the incidence of heat source/ sink were considered by Dessie and Kishan [16].
Brownian motion and thermophoresis influences on a nanofluid over a nonlinearly permeable stretching sheet have been analyzed by Falana et al. [17]. Ibrahim and Shankar [18]numerically examinedunsteadylaminar viscous boundary layer flow and heat transport in an incompressible fluid over a stretching sheet. They explained that the stretching velocity of time-dependent and surface temperature causes the flow and temperature unsteadiness. Abd El- Aziz and Yahaya[19] presented the joint effect of thermal and concentration diffusions in unsteady MHD free convection flow past a moving plate maintained at constant heat flux and embedded in a viscous fluid-saturated porous medium. A flow on a boundary layer and the influence of heat and mass transfer in a viscoelastic electrically conducting fluid through a porous medium subject to a magnetic transverse field in the incidence of chemical reaction and heat source/sink has been studied by Nayak et al. [20]. In their analysis, they accomplished the field of temperature for both (PST) and (PHF) results. Swain et al. [21] have made an effort to study the impact of heat and mass transport in a boundary layer MHD flow of a viscous electrically conducting fluid through a porous medium over a stretching exponentially sheet.

Most of the exceeding studies are limited to boundary layer flow and transmission of heat in Newtonian fluids. Nevertheless, because of the growingsignificance of nanofluids, a marvelous amount of concern has been given to the study of nanofluids

convective transport in recent years. The word 'nanofluid' invented by Choi [22]explains a liquid stretching sheet, it was formed by suspending nanoparticles into a base fluid. The nanoparticles that are used commonly are metals like copper, aluminum, iron, and gold and the base fluids usually used are like glycol, water and toluene or oil. Later on, several authors studied Nanofluids. Ebaid et al. [23] analyzed the effect of velocity slip boundary on the flow and heat transfer of Cu-Water and TiO_2-Water Nanofluids in the presence of a magnetic field. They obtained that the Cu-Water is slower than the TiO_2-Water Nanofluid for both cases of the stretching/shrinking sheets. However, the temperature of the Cu-Water Nanofluid is always higher than the temperature of the TiO_2-Water Nanofluid. Ibrahim [24]inspectedNanofluid stagnation MHD flow and heat transportof a melting past a stretching sheet. He found that an increase of melting heat transfer and magnetic parameter reduces both the skin friction coefficient and Sherwood number. Anki Reddy et al. [25]focused their study on the numerical solution of MHD boundary layer slip flow of a Maxwell Nanofluid over an exponentially stretching surface with convective boundary condition. Daniel et al. [26]considered the concurrentimpact of magnetic and applied electric fields, thermal stratification, thermal radiation, viscous dissipation and heating of Joules are numerically on a boundary layer flow of electrically conducting Nanofluid over a nonlinearly stretching sheet with variable thickness.

Bal Reddy et al. [32] investigated numerically the radiation effects on MHD fluid flow of a nanofluid past an exponential stretching sheet in a porous medium. Reddy et al. [27]also inspecteda flow on a boundary layer with MHDand the transport of heat and mass for Williamson Nanofluid over a stretching sheet with variable thickness and variable thermal conductivity underradiation influences.The effects of Soret and Dufour are essential when density variationsoccur in the flow regime.

The impact of Dufour and Soret on free convective heat and mass transport over a stretching surface with suction or injection were investigated by Ahmed [28]. He established that the coefficient of skin friction and the local Nusselt number raises with Dufour numbers but reduces with the Soret influence. Alternatively, an increase of Dufour numbers enhances the local Sherwood number, but it decreases with an increase of Soret number.On observingthat in almost above literature the mass transfer effects for the considered nano-liquids are ignored. Hence, we have investigated heat and mass transfer characteristics of copper and silver nano-liquids due to a stretching sheet in the presence of a uniform heat source for which an OHAM is used.

II. FORMULATION OF THE PROBLEM

An incompressible two-dimensional laminar steady nanoliquidflow over a stretching sheet is reflected on. The origin of the system is situated at the slit where the sheet is drawn. The stretching continuous surface is taken in thex −axis direction and the y −axis is consideredperpendicular to the surface of the sheet.The liquids are considered to be a water-based nanoliquidhaving two different types of nanoparticles: copper and Silver nano-particles. It is thoughtthat the base fluid and the nanoparticles are found to bein thermal equilibrium and between them no slip exists. The nano-fluid thermophysical properties are given in Table-1 with the above hypothesis, the governing boundary layer equations of the nanoliquid flow, the heat and the concentration fields can be inscribed in dimensional form.

$$\frac{\partial u}{\partial x}+\frac{\partial v}{\partial y}=0 \tag{1}$$

$$u\frac{\partial u}{\partial x}+v\frac{\partial v}{\partial y}=\frac{\mu_{nf}}{\rho_{nf}}\frac{\partial^2 u}{\partial y^2} \tag{2}$$

$$u\frac{\partial T}{\partial x}+v\frac{\partial T}{\partial y}=\alpha_{nf}\frac{\partial^2 T}{\partial y^2}+\frac{Q}{(\rho c_p)_{nf}}(T-T_\infty) \tag{3}$$

$$u\frac{\partial C}{\partial x}+v\frac{\partial C}{\partial y}=D\frac{\partial^2 C}{\partial y^2}+D_1\frac{\partial^2 T}{\partial y^2} \tag{4}$$

Where u and v are the velocity components in the x and y −directions respectively,ρ is the fluid density,T is the temprature, C is the concentration,C_∞ is the concentration of the fluid far from the sheet. C_p is the specific heat at constant pressure, D is thediffusivity of specifies, and D_1 is the coefficient that indicates the contribution to mass flux through temperature gradient:

The boundary conditions for Eqs. (1)-(4) are assumed in the form:

$$\left.\begin{aligned} u=u_w=bx, v=0, T=T_w=T_\infty+A\left(\frac{x}{l}\right)^2, \\ C=C_w=C_\infty+Q\left(\frac{x}{l}\right)^2 \ at\ y=0 \\ u\to 0, T\to T_\infty, C\to C_\infty as\ y\to\infty, \end{aligned}\right\} \tag{5}$$

Where A, Q,and b are constants,l is the characteristic length,T_∞ is the fluidtemperature far from the sheeThe nano-fluid effective dynamic viscosity was given by Brinkman[29] as$\mu_{nf}=\frac{\mu_f}{(1-\phi)^{2.5}}$ (6)

Where ϕ is the solid volume fraction of the nano-particles. The effective density, ρ_{nf}, thermal diffusivity,α_{nf} and the heat capacitance of the nano fluid are given by:

$$\rho_{nf}=(1-\phi)\rho_f+\phi\rho_s, \tag{7}$$

$$\alpha_{nf}=\frac{k_{nf}}{(\rho c_p)_{nf}}, \tag{8}$$

$$(\rho c_p)_{nf}=(1-\phi)(\rho c_p)_f+\phi(\rho c_p)_s \tag{9}$$

The nanofluids thermal conductivity restricted to spherical nano particles is estimated by the Maxwell-Garnett model(see Max-well Garnett [30] and Guerin etal.[31]).

$$k_{nf} = k_f \left[\frac{k_s+2k_f-2\phi(k_f-k_s)}{k_s+2k_f+\phi(k_f-k_s)}\right] \quad (10)$$

In Eqs. (7)-(10), the subscripts n_f, f and$s$ denote the thermo physical properties of the nano-fluid, base fluid and nano-solid particles, respectively.

The continuity equation (1) is satisfied by introducing a stream function $\psi(x,y)$ such that

$$u = \frac{\partial\psi}{\partial y}, \quad v = -\frac{\partial\psi}{\partial x} \quad (11)$$

The following Similarity variables are also introduced:

$$\left.\begin{array}{c} u = bxf'(\eta), \qquad v = -\sqrt{bv_f}\, f(\eta) \\ T = T_\infty + (T_w - T_\infty)\theta(\eta), C = C_\infty + (C_w - C_\infty)\beta(\eta) \\ \eta = \sqrt{\frac{b}{vf}}\, y, \quad \psi = \sqrt{v_f b}\, xf \end{array}\right\} \quad (12)$$

Where ηis the similarity variable,f(η) is the dimensionless stream function, θ(η) is the dimensionless temperature and β(η) is the dimensionless concentration.

on using Eqs. (6),(7), (8), (9), (10) and (12), Eqs. (2)-(4) transform in to the following two-point boundary value problems.

$$f''' - \phi_1\left[f'^2 - ff''\right] = 0 \quad (13)$$

$$\theta'' - \mathrm{Pr}\frac{k_f}{k_{nf}}\phi_3[2f'\theta - f\theta' - \delta\theta] = 0 \quad (14)$$

$$\beta'' - \mathrm{Sc}[2f'\beta - f\beta'] + \mathrm{Sr}\theta'' = 0 \quad (15)$$

The corresponding boundary conditions are:

$$f(0) = 0, f'(0) = 1, f'(\infty) \to 0 \quad (16)$$

$$\theta(0) = 1, \theta(\infty) \to 0, \quad (17)$$

$$\beta(0) = 1, \beta(\infty) \to 0, \quad (18)$$

The non dimensional constants appearing in Eqs. (13)-(15) are the Prandtl number Pr, the Schmidt number Sc, the Soret number Sr and the heat generationparameterδ.

They are respectively defined as:

$$\mathrm{Pr} = \frac{v_{f(\rho c_p)f}}{k_f}, \quad \mathrm{Sc} = \frac{v_f}{D}, \quad \mathrm{Sr} = \frac{D_1(T_w - T_\infty)}{D(C_w - C_\infty)}, \text{and}\delta = \frac{Q}{b(\rho c_p)_{nf}}$$

Where

$$\left\{\begin{array}{l} \phi_1 = (1-\phi)^{2.5}\left[1 - \phi + \phi\left(\frac{\rho_s}{\rho_f}\right)\right] \\ \phi_3 = 1 - \phi + \phi\frac{(\rho c_p)_s}{(\rho c_p)_f}, \end{array}\right. \quad (19)$$

III. SKIN FRICTION, HEAT AND MASS TRANSFER COEFFICIENTS

The engineering parameterscontained in heat and mass transport problems are the skin friction coefficient C_f , the local Nusselt number Nu_x and the local Sherwood number Sh_x. These engineering parameters characterizes the surface drag, wall heat and mass transfer rates respectively. Thus, the shearing stress at the surface of the wall τ_w is given by

$$\tau_w = -\mu_{nf}\left[\frac{\partial u}{\partial y}\right]_{y=0} = -\frac{1}{(1-\phi)^{2.5}}\rho_f\sqrt{v_f b^3}\, xf''(0) \quad (20)$$

where μ_{nf} is the coefficient of viscosity. The skin friction coefficient is defined as$C_f = \frac{2\tau_w}{\rho u^2{}_w}$ (21)

and using Eq. (20) in Eq. (21) we obtain $C_f(1-\phi)^{2.5}\sqrt{Re_x} = -2f''(0)$ (22)

The heat transfer rate at the surface flux at the wall is given by

$$q_w = -k_{nf}\left[\frac{\partial T}{\partial y}\right]_{y=0} = -k_{nf}A\left(\frac{x}{l}\right)^2\sqrt{\frac{b}{v_f}}\theta'(0) \quad (23)$$

where k_{nf} is the Nanofluids thermal conductivity. The Nusselt number is defined as:$Nu_x = \frac{x}{k_f}\frac{q_w}{T_w - T_\infty}$ (24)

Using Eq. (23) in Eq. (24), the dimensionless wall heat transfer rate is obtained as $\frac{Nu_x}{\sqrt{Re_x}}\left(\frac{k_f}{k_{nf}}\right) = -\theta'(0)$ (25)

The mass flux at the wall surface is given by $J_w = -D\left[\frac{\partial C}{\partial y}\right]_{y=0} = -D\left(\frac{x}{l}\right)^2\sqrt{\frac{b}{v_f}}\beta'(0)$ (26)

and the Sherwood number is defined as $Sh_x = \frac{x}{D}\frac{J_w}{C_w - C_\infty}$ (27)

Using (26) in (27) the dimensionless wall mass transfer rate is obtained as$\frac{Sh_x}{\sqrt{Re_x}} = -\beta'(0)$ (28)

In Eqs. (22),(25) and (28), Re_x represents the local Reynolds number defined as:$Re_x = \frac{xu_w}{v_f}$

IV. SOLUTION BY OHAM

Pursuing the basic theories and procedure of OHAM as done by Nandeppanavar et al.[33]. The solution of Eq (13) -(15) with respect to the corresponding boundary conditions (16) to (18) can be explainedby optimal homotopy asymptotic method as:
Using the OHAM procedure we can write Eqs. (13),(14) and (15) respectively as:

$$\left.\begin{aligned}(1-p)(f''+f')-H_1(p)[\left(\left(f'''-\phi_1\left(f'^2-ff''\right)\right)-(f''+f')\right]=0,\\ (1-p)(\theta'+\theta)-H_2(p)\left[\left(\theta''-Pr\frac{k_f}{k_{nf}}\phi_3(2f'\theta-f\theta'-\delta\theta)\right)-(\theta'+\theta)\right]=0,\\ (1-p)(\beta'+\beta)-H_3(p)[(\beta''-Sc(2f'\beta-f\beta')+Sr\theta'')-(\beta'+\beta)]=0\end{aligned}\right\} \quad (29)$$

Evidently when $p=0$ and $p=1$

$$\psi(\eta,0)=v_0(\eta) \quad \text{and} \psi(\eta,1)=v(\eta) \quad (30)$$

Thus, as $p$increases from *0 to 1*, the solution varies from $v_0(\eta)$ *to* $v_1(\eta)$. for $p=0$, we can write

$$L(v_0(\eta))+g(\eta)=0, B(v_0)=0, \quad (31)$$

The auxiliary equation H(p) is chosen as:

$$H(p)=pC_1+p^2C_2+p^3C_3+\cdots, \quad (32)$$

Where C_1, C_2, C_3 ...are constants.
In the same way, the auxiliary equations for the momentum, heat transfer and mass transfer shall be explains of(31) as:

$$\left.\begin{aligned}H_1(p)=pC_{11}+p^2C_{12}+\cdots\\ H_2(p)=pC_{21}+p^2C_{22}+\cdots\\ H_3(p)=pC_{31}+p^2C_{32}+\cdots\end{aligned}\right\} \quad (33)$$

The expansion of$\phi(\eta, p)$ in series with respect to p can be expressed as:

$$\psi(\eta,p,C)_i=v_0(\eta)+\sum_{k\geq1}v_k(\eta,C_i)p^k, i=1,2,3\ldots \quad (34)$$

Now following the method and substituting (33) into (29) we can write:
The Zeroth order as

$$\left.\begin{aligned}p^0: \quad f''_0+f'_0=0\\ f_0(0)=0, f'_0(0)=1\\ \theta'_0+\theta_0=0\\ \theta_0(0)=1\\ \beta'_0+\beta_0=0\\ \beta_0(0)=1\end{aligned}\right\} \quad (35)$$

The first order:

$$\left.\begin{aligned}p^1: \quad -f'_0+C_{11}f'_0-f''_0+C_{11}f''_0-C_{11}f'''_0+f'_1+f''_1+C_{11}f'^2_0\phi_1-C_{11}f_0f''_0\phi_1=0\\ f_1'(0)=0, f_1(0)=0,\\ -\theta_0+C_{21}\theta_0-\theta'_0+C_{21}\theta'_0-C_{21}\theta''_0+\theta_1+\theta'_1+\frac{2C_{21}f'_0\theta_0K_fP_r\phi_3}{K_{nf}}-\frac{C_{21}f_0\theta'_0K_fp_r\phi_3}{K_{nf}}-\frac{C_{21}\theta_0K_fp_r\delta\phi_3}{K_{nf}}=0\\ \theta_1(0)=0\\ -\beta_0+C_{31}\beta_0-\beta'_0+C_{31}\beta'_0-C_{31}\beta''_0+\beta_1+\beta'_1+2C_{31}f'_0\beta_0Sc-C_{31}f_0\beta'_0Sc-C_{31}\theta''_0Sr=0\\ \beta_1(0)=0\end{aligned}\right\} \quad (36)$$

The second order:

$$\begin{aligned}p^2: \quad & C_{12}f'_0+C_{12}f''_0-C_{12}f'^2_0-f'_1+C_{11}f'_1-f''_1+C_{11}f''_1-C_{11}f'^2_1+f'_2+f''_2+C_{12}f'^2_0\phi_1-C_{12}f_0f''_0\phi_1\\ & -C_{11}f''_0f_1\phi_1+2C_{11}f'_0f'_1\phi_1-C_{11}f_0f''_1\phi_1=0\\ & f_2'(0)=0, f_2(0)=0\\ & C_{22}\theta_0+C_{22}\theta'_0-C_{22}\theta''_0-\theta_1+C_{21}\theta_1-\theta'_1+C_{21}\theta'_1-C_{21}\theta''_1+\theta_2+\theta'_2+\frac{2C_{22}f'_0\theta_0k_fPr\phi_3}{k_{nf}}+\frac{2C_{21}f'_1\theta_0k_fPr\phi_3}{k_{nf}}\\ & -\frac{C_{22}f_0\theta'_0k_fPr\phi_3}{k_{nf}}-\frac{C_{21}f_1\theta'_0k_fPr\phi_3}{k_{nf}}+\frac{2C_{21}f'_0\theta_1k_fPr\phi_3}{k_{nf}}-\frac{C_{21}f_0\theta'_1k_fPr\phi_3}{k_{nf}}-\frac{C_{22}\theta_0k_fPr\phi_3\delta}{k_{nf}}\\ & -\frac{C_{21}\theta_1k_fPr\phi_3\delta}{k_{nf}}=0,\\ & \theta_2(0)=0\\ & C_{32}\beta_0+C_{32}\beta'_0-C_{32}\beta''_0-\beta_1+C_{31}\beta_1-\beta'_1+C_{31}'_1-C_{31}\beta''_1+\beta_2+\beta'_2+2C_{32}f'_0\beta_0Sc+2C_{31}f'_1\beta_0Sc-C_{32}f_0\beta'_0Sc\\ & -C_{31}f_1\beta'_0Sc+2C_{31}f'_0\beta_1Sc-C_{31}f_0\beta'_1Sc-C_{32}\beta''_0Sr-C_{31}\beta''_1Sr=0\end{aligned}$$

$$\beta_1(0)=0 \quad (37)$$

Hence, we get general solution of Eq. (33) as:

$$^{(m)}_{v}(\eta,C_i)=v_0(\eta)+\sum_{k=1}^{m}v_k(\eta,C_i), i=1,2,3\ldots.m. \quad (38)$$

One can obtain the zeroth order and first order solution with corresponding boundary conditions, respectively as:

$$\left.\begin{aligned} f_0(\eta) &= 1 - e^{-\eta} \\ \theta_0(\eta) &= e^{-\eta} \\ \beta_0(\eta) &= e^{-\eta} \end{aligned}\right\} \quad (39)$$

$$\left.\begin{aligned} f_1 &= -C_{11}e^{-\eta}(-1+\phi_1)(-1+e^{\eta}-\eta) \\ \theta_1 &= \frac{C_{21}e^{-2\eta}(k_f Pr\phi_3 - e^{\eta}k_f Pr\phi_3 + e^{\eta}k_{nf}\eta - e^{\eta}k_f Pr\phi_3\eta + e^{\eta}k_f Pr\phi_3\eta\delta)}{k_{nf}} \\ \beta_1 &= -C_{31}e^{-2\eta}(-Sc + e^{\eta}Sc - e^{\eta}\eta + e^{\eta}\eta Sc - e^{\eta}\eta Sr) \end{aligned}\right\} \quad (40)$$

Similarly, we can obtain second order solutions too, for brevity, the solutions for $f_2(\eta), \theta_2(\eta)$ *and* $\beta_2(\eta)$ are not presented here. Consequently, solutions for the equation of momentum, heat transfer and mass transfer (up to second-order terms) are given by

$$\left.\begin{aligned} f(\eta) &= f_0(\eta) + f_1(\eta) + f_2(\eta) \\ \theta(\eta) &= \theta_0(\eta) + \theta_1(\eta) + \theta_2(\eta) \\ \beta(\eta) &= \beta_0(\eta) + \beta_1(\eta) + \beta_2(\eta) \end{aligned}\right\} \quad (41)$$

The substitution of the values of $f(\eta)$, $\theta(\eta)$ *and* $\beta(\eta)$ from (48) in to equations (13), (14) and (15), the residuals can be obtained as:

$R_1(\eta, C_{11}, C_{12}), R_2(\eta, C_{21}, C_{22})$ *and* $R_3(\eta, C_{31}, C_{32})$, Subsequently we can obtain the Jacobians J_1, J_2 *and* , J_3 as follows:

$$J_1(\eta, C_{11}, C_{12}) = \int_0^b {R_1}^2(\eta, C_{11}, C_{12})d\eta \quad (42)$$

$$J_2(\eta, C_{21}, C_{22}) = \int_0^b {R_2}^2(\eta, C_{21}, C_{22})d\eta \quad (43)$$

$$J_3(\eta, C_{31}, C_{32}) = \int_0^b {R_3}^2(\eta, C_{31}, C_{32})d\eta \quad (44)$$

With these known constants, approximate solution of the problem(to order m) can be determined very easily.

V. RESULTS AND DISCUSSION

In the analytic solutions, the effects of nanoparticle volume fraction, heat generation parameter,Schmidt number and Soret number on heat and mass transfer characteristics of nanofluid were reflected on. Two types of nanoparticles, specifically, Copper and Silver, with water as the base fluid with a constant Prandtl number $Pr = 6.2$,were taken into account. The transformednonlinear ordinary differential equations (13)-(15) subject to the boundary conditions (16-18) were solved analytically using the optimal homotopy asymptotic method(OHAM). The profiles of velocity, temperature, and concentration were acquired and we practiced the results to compute the coefficient of skin friction, the local Nusselt number, and local Sherwood number. The analytical results were discussed for distinct values of the parameters graphically and in tabular form. The analytic method was validated by comparing withearlier published journals by Yohannes and Danel [34] and Hamad [35]. As revealed in Table-2 the results are found in a nice agreement.The coefficients of skin friction for distinct values of volume size of the nanoparticles $\phi$and when $Pr = 6.2,\ Sc = 1,\ Sr = 0.2, \delta = 0.1$ are given in Table-2.

The coefficients of heat transfer are shown in Table-3 for different Prandtl numbers. It is clear that the heat transfer coefficient increases with increasing Prandtl numbers**.** The results areattained in an excellent agreement with the previousresults by Kameswaran[10]. An enhancement in the values of Prandtl number reveals that the thermal diffusivity is dominated by momentum diffusivity. Hence, the rate of heat transfer at the surface raises with an increment of Prandtl number.

Table-1

Thermo physical properties of water, copper and silver nano-particles at 300^0k (see Oztop and Abu-Nada [35]).

Physical Quantity	properties			
	$\rho(\frac{kg}{m^3})$	$k(\frac{w}{m\,k})$	$\beta_{np} x10^5(k^{-1})$	$c_p(\frac{j}{kg\,k})$
water	997.1	0.613	21	4179
Copper(Cu)	8933	401	1.67	385
Siliver(Ag)	10500	429	1.89	235

Table - 2

Comparison of the skin friction coefficient $-f''[0]$ for different values of Nanoparticle volume fraction($\boldsymbol{\phi}$)**,**when magnetic parameter M = 0 and Prandtl number $Pr = 6.2$.

M	$\boldsymbol{\phi}$	[36]		[33]		Present results	
		Cu-water	Ag-water	Cu-water	Ag-water	Cu-water	Ag-water
0	0.05	1.10892	1.13966	1.1089	1.1397	1.10885	1.13951
	0.1	1.17475	1.22507	1.1747	1.2251	1.17446	1.22447
	0.15	1.20886	1.27215	1.2089	1.2722	1.20838	1.2711
	0.2	1.21804	1.28979	1.2180	1.2898	1.21749	1.28852

Table-3

Comparison of the values of wall Temperature gradient $-\theta'(0)$ for different values of Prandtl numbers.

Results	*P r=0.72*	*Pr = 1*	*Pr = 3*
Kameswaran [8]	1.08852	1.33333	2.50973
Present	1.09039	1.33333	2.49531

The volume size of nanoparticle ϕinfluence on the velocity, temperature and concentration profiles for both nanofluids is shown by Fig.1-3. It is indicated that as the nanoparticle volume fraction raises, the *Cu*-water and *Ag*-water nanoliquid velocity reduces. We also saw that the axial velocity in the case of a *Cu*-water nanoliquid is relatively greater than *Ag*-water nanoliquid. As it is revealed in Fig.2, the increment of the volume fraction of nanoparticles enhances the thermal conductivity of the nanoliquid and in turn results in the thermal boundary layer to be thickening. It is also noticed that the distribution of temperature is higher in *Ag*-water nanoliquid than in *Cu*-water nanoliquid. This is apredictable result because *Ag* is a good heat conductor and electricity. In fig. 3, the nanoparticle volume size increment made the thickness of the concentration boundary layer enlarged for both types of nanoliquids considered.

The coefficient of skin friction $-f''(0)$ as a function of the nanoparticle volume size ϕ is demonstrated by Fig. 4. We watched that for clear fluid,$\phi = 0$, the coefficient of skin friction value is unity, a Crane's [9] problem standard result. An enlargement of ϕ enlarges the coefficient of skin friction monotonically to a maximum value before declining. The findings explained relating to the coefficient of skin friction hold for the two nanoliquids. For *Cu*-water nanoliquid the highest value of the skin friction is accomplished at a smaller value of ϕ in comparison with an *Ag*-water nanoliquid. Supplementary, the *Cu*-water nanoliquid display slower drag to the flow as compared to the *Ag*-water nanoliquid. The non-dimensional rate of wall heat transfer$-\theta'(0)$ and non-dimensional rate of wall mass transfer $-\beta'(0)$ are detained as a function of the volume size of the nanoparticleϕin Fig. 5 and Fig. 6, respectively. We observed that $-\theta'(0)$ is a decreasing function of ϕwhile the opposite is true in the case of $-\beta'(0)$. The Cu–water nanofluid exhibits higher wall heat and mass transfer rates as compared to anAg–water nanoliquid. The presence of nanoparticles tends to reduce the wall heat transfer rate and to increase the wall mass transfer rates.

Fig. 7 and 8 illustrate the influence of heat generation parameter δ on the temperature profile and concentration profile in the case of Cu-water and Ag-water nanoliquids. We saw that the temperature field increases for both cases of nanoliquids with increasing the values of the heat generation parameter δ. It is explained that the temperature profileofAg-water is greater than that of Cu-water nanofluids. Increasing the values of the heat generation parameter δ increases the thermal conductivity of nanofluid and the thickening of the thermal boundary layer. We also watched that the concentration profile decreases for both cases of nanoliquids with increasing the values of the heat generation parameter δ.

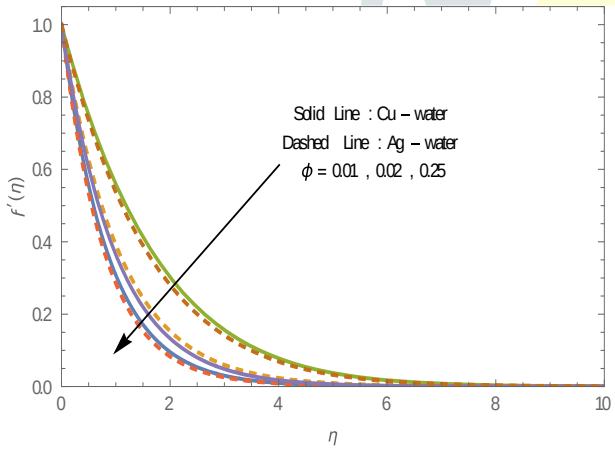

Figure 1: Velocity profile as a function of ϕ.

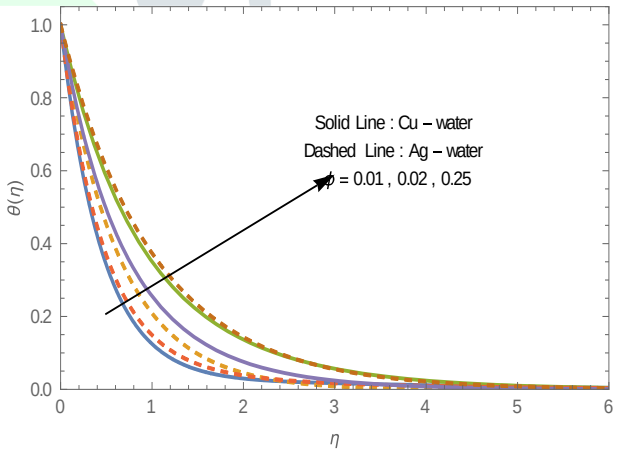

Fig. 2: Temperature profile as a function of ϕ when $\delta = 1 and\ Pr = 6.2$.

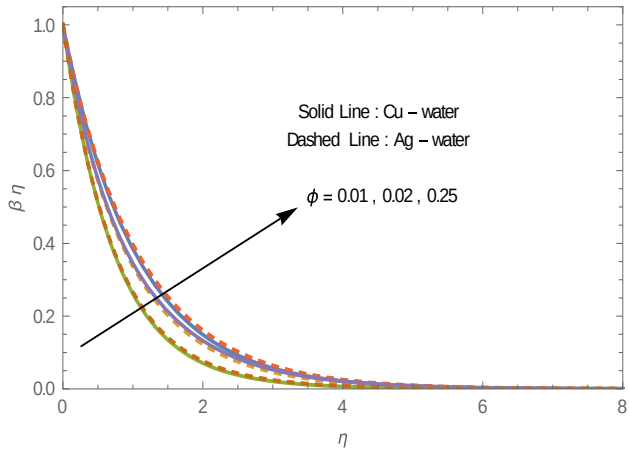

Fig. 3: Concentration profile as a function of ϕ when $\delta = 1, Pr = 6.2, Sc = 1 Sr = 0.2$

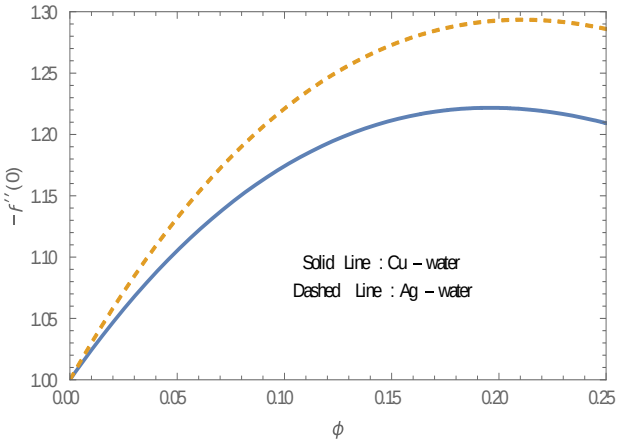

Fig. 4: Coefficient of skin friction as a function of ϕ when $Sc = 1, Sr = 0.2, \delta = 1 and\ Pr = 6.2.$

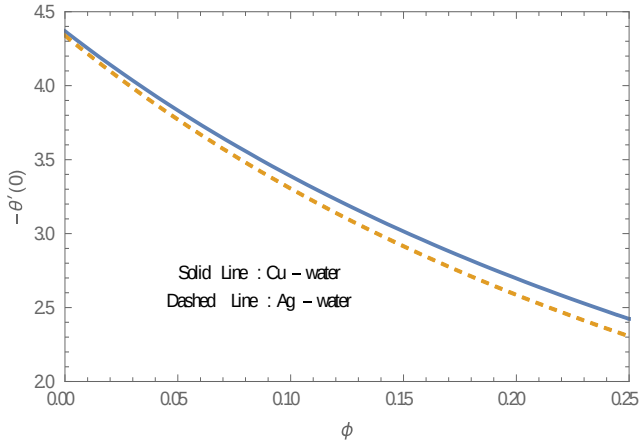

Fig. 5: Heat transfer coefficient as a function of ϕ when $Sc = 1, Sr = 0.2, \delta = 1 and\ Pr = 6.2$

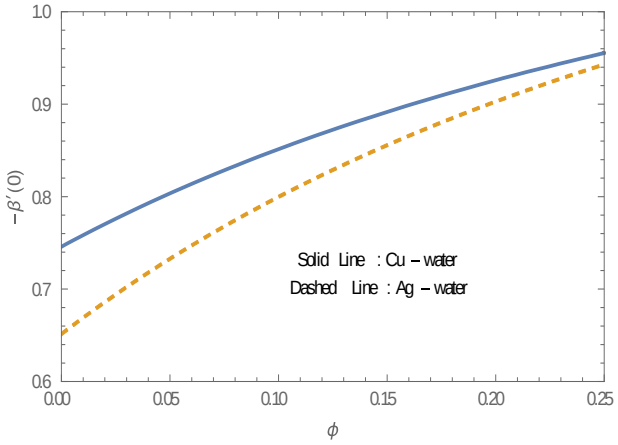

Fig. 6: Mass transfer coefficient as a function of ϕ when $Sc = 1, Sr = 0.2, \delta = 1 and\ Pr = 6.2..$

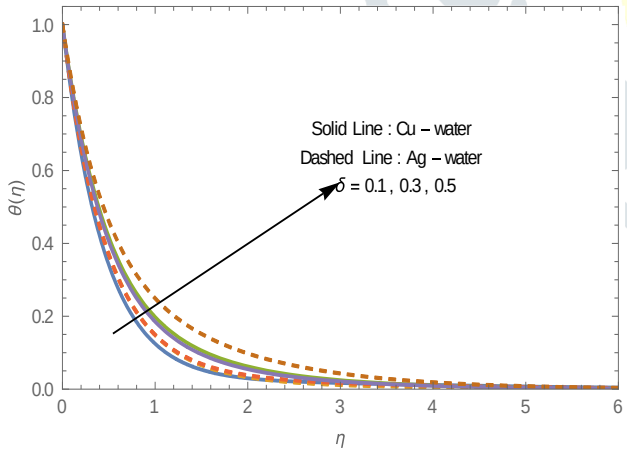

Fig. 7: Temprature profile with variation of δ for $Sc = 1, Sr = 0.2, \phi = 0.3 and\ Pr = 6.2.$

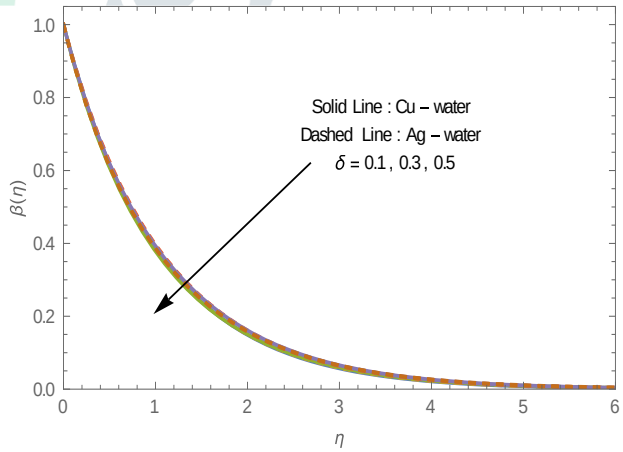

Fig. 8: Concentration profile with variation of δ $for\ Sc = 1, Sr = 0.2, \phi = 0.3 and\ pr = 6.2.$

Fig. 9 Shows that the temperature profile in both cases of the nanoliquids decreases as the Prandtl number increases. And we found that the temperature profile of *Ag*-water is higher than that of *Cu*-water. Fig.10reveals that the concentration profile for both cases of nanoliquids increases as the Prandtl number increases. This shows that the increase of the Prandtl number increases the thickening of the boundary layer of the concentration profile. And the concentration profile of *Ag*-water is higher than that of *Cu*-water. Fig. 11 illustrates the effect of the Soret number Sron the concentration profile in the case of Cu-water and Ag_ water nanoliquids. As the Soret number increases, the boundary layer thickness of the concentration ofboth nanoliquids increases. It is described that the concentration increment of Ag–water is more than that of Cu–water nanoliquid.

We note from Eqs. (14) and (15) that the functions $\theta$and $\beta$are partially despaired, hence the Schmidt number $Sc$and the Soret number Srhave no influence on heat transport. Fig. 12displays the Schmidt number Scimpact on concentration profiles in the

case of Cu-water and Ag-water nanoliquids. As the values ofthe Schmidt number enlarges the concentration profiles of both nanoliquidslessens. We observed that the concentration increment of Ag −water is more than that ofCu–water.

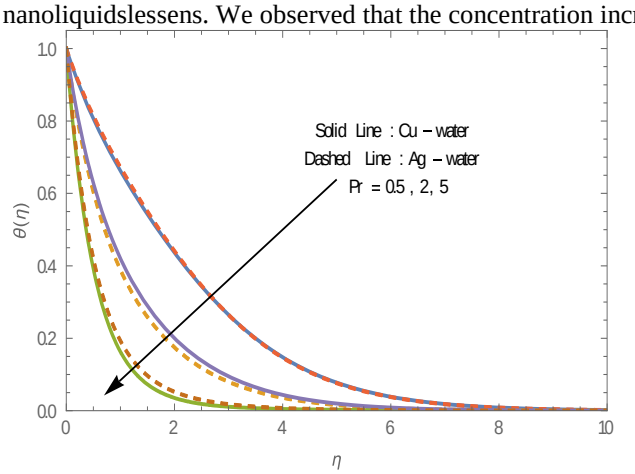

Fig. 9: Temperature profile with variation of Pr for $Sc = 1, Sr = 0.2, \phi = 0.3$ and $\delta = 0.1$.

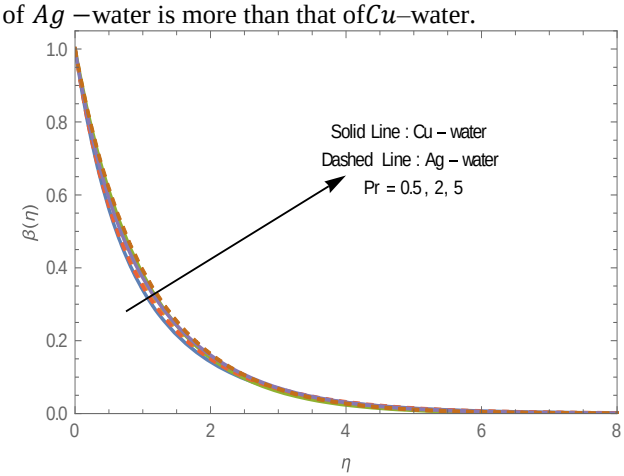

Fig. 10: Concentration profile with variation of Pr for $Sc = 1, Sr = 0.2, \phi = 0.3$ $and\delta = 0.1$.

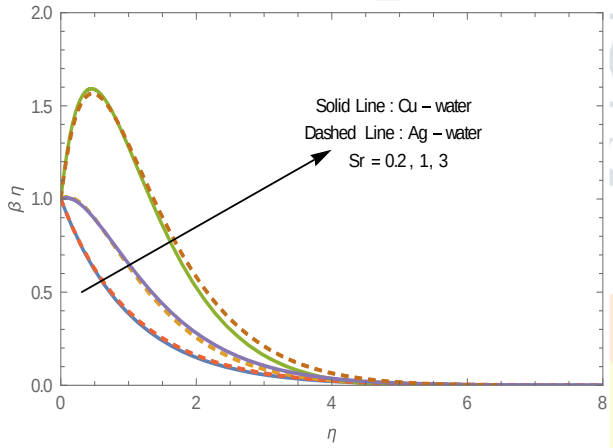

Fig.11. The effect of Sr on the concentration profile when $Sc = 1, \phi = 0.3, \delta = 0.1 and\ Pr = 6.2$.

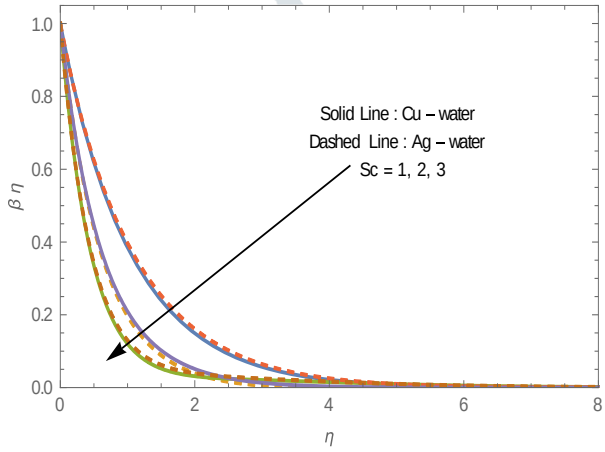

Fig.12. The effect of Sc on the concentration profile $when\ Sr = 0.2, \phi = 0.3, \delta = 0.1 and\ Pr = 6.2$.

VI. CONCLUSION

This paper presents the problem of heat and mass transfer in the flow of nanoliquiddue to a stretching sheet in the occurrence of heat generation. The governing nonlinear partial differential equations were transformed into ordinary differential equations using the similarity approach and solved analytically using the OHAM. Two types of nanoliquids were considered, *Cu*-water and *Ag*-water, and our results revealed, among others, the following.

- Cu-water shows a thicker velocity boundary than Ag-water nanoliquid. The thickness of the velocity boundary layer reduces with an increment of the volume size of nanoparticles.
- *Cu*-water nanoliquidthickness of the thermal boundary layer is less than *Ag*-water nanoliquid. An increase of ϕ enlarges the thermal boundary layer thickness.
- The boundary layer thickness of concentration for*Ag*-water nanoliquidisfaintlymore than *Cu*-water nanoliquid.
- The increment of *Pr*enhances concentration boundary layer thickness, while it reduces with increasing the values of the *Sc*.
- The coefficient of skin friction increases with the nanoparticle volume fraction increment; the *Ag*-water nanoliquid showshigher skin friction than *Cu*-water nanoliquid.
- The rate of heat transfer at the plate surface declines with rising the volume size ofthe nanoparticle. The *Cu*-water nanoliquid has a higher rate of heat transfer rate than the *Ag*-water nanoliquid.
- The mass transfer rate at the plate surface raises with an increment of the nanoparticle volume fraction, The *Ag*-water nanoliquid has higher rate of mass transfer than the *Cu*-water nanoliquid.
- We have compared the values of skin friction and heat transfer rate for some particular parameters, it is observed that our results are in very good agreement with earlier results. These values are tabulated in the table-2 and Table-3.

REFERENCES

1. L. Crane, "Flow past a stretching plate," *Zeitschrift fur Angew. Mathe-matik und Phys. ZAMP*, vol. 21, no. 4, pp. 645–647, 1970.
2. I. S. Awaludin, A. Ishak, and I. Pop, "On the Stability of MHD Boundary Layer Flow over a Stretching/ Shrinking Wedge," *Sci. Rep.*, 2018.
3. N. F. M. Noor and I. Hashim, "ADM solution for MHD boundary layer flow over a nonlinearly stretching sheet in the presence of viscous dissipation," *Am. Inst. Phys.*, p. 030019 (1-7), 2016.
4. R. G. Abdel-Rahman, "MHD Slip Flow of Newtonian Fluid past a Stretching Sheet with Thermal Convective Boundary Condition, Radiation, and Chemical Reaction," *Math. Probl. Eng.*, 2013.
5. Krishnendu Bhattacharyyaa Tasawar Hayatb and A. Alsaedic, "Analytic solution for magnetohydrodynamic boundary layer flow of Casson fluid over a stretching/shrinking sheet with wall mass transfer," *Chin. Phys. B*, vol. 22, no. 2, p. 024702(1-6), 2013.
6. M. Reza, R. Chahal, and N. Sharma, "Radiation Effect on MHD Casson Fluid Flow over a Power-Law Stretching Sheet with Chemical Reaction," *Int. J. Chem. Mol. Eng.*, vol. 10, no. 5, pp. 585–590, 2016.
7. I. Ullah, K. Bhattacharyya, S. Shafie, and I. Khan, "Unsteady MHD Mixed Convection Slip Flow of Casson Fluid over Nonlinearly Stretching Sheet Embedded in a Porous Medium with Chemical Reaction, Thermal Radiation, Heat Generation/Absorption and Convective Boundary Conditions," *PLoS One*, 2016.
8. K. Ahmad and A. Ishak, "Magnetohydrodynamic (MHD)Jeffrey fluid over a stretching vertical surface in a porous medium," *Propuls. Power Res.*, vol. 6, no. 4, pp. 269–276, 2017.
9. Z. Shah, E. Bonyah, S. Islam, W. Khan, and M. Ishaq, "No TitleRadiative MHD thin film flow of Williamson fluid over an unsteady permeable stretching sheet," *Heliyon*, vol. 4, 2016.
10. P. . Kameswaran, M. Narayana, P. Sibanda, and P. V. S. . Murthy, "Hydromagnetic nanofluid flow due to a stretching or shrinking sheet with viscous dissipation and chemical reaction effects," *Int. J. Heat Mass Transf.*, vol. 55, pp. 7587–7595, 2012.
11. C. S. . Raju, N. Sandeep, M. J. Babu, and V. Sugunamma, "Dual solutions for three- dimensional MHD flow of a nanofluid over a nonlinearly permeable stretching sheet," *Alexandria Eng. J.*, vol. 55, pp. 151–162, 2016.
12. S. Jena, S. R. Mishra, and G. C. Dash, "Chemical Reaction Effect on MHD Jeffery Fluid Flow over a Stretching Sheet Through Porous Media with Heat Generation/Absorption," *Int. J. Appl. Comput. Math*, vol. 2016.
13. A. Gizachew and B. Shankar, "Analytical Solutions of an MHD Heat and Mass Transfer of a Jeffery Fluid Flow over a Stretching Sheet with the Effect of Slip Velocity," *Adv. Appl. Sci.*, vol. 3, no. 3, pp. 34–42, 2018.
14. S. A. Gaffar, V. R. Prasad, and E. K. Reddy, "Computational study of Jeffrey's non-Newtonian fluid past a semi-infinite vertical plate with thermal radiation and heat generation/absorption," *Ain Shams Eng. J.*, vol. 8, pp. 277–294, 2017.
15. F. M. Ali, R. Nazar, N. M. Arifin, and I. Pop, "Dual solutions in MHD flow on a nonlinear porous shrinking sheet in a viscous fluid," *Bound. Value Probl.*, 2013.
16. H. Dessie and N. Kishan, "MHD effects on heat transfer over stretching sheet embedded in porous medium with variable viscosity, viscous dissipation and heat source/sink," *Ain Shams Eng. J.*, vol. 5, pp. 967–977, 2014.
17. A. Falana, O. A. Ojewale, and T. B. Adeboje, "Effect of Brownian Motion and Thermophoresis on a Nonlinearly Stretching Permeable Sheet in a Nanofluid," *Adv. Nanoparticles*, vol. 5, pp. 123–134, 2016.
18. W. Ibrahim and B. Shanker, "No TitleUnsteady Boundary Layer Flow and Heat Transfer Due to a Stretching Sheet by Quasilinearization Technique," *World J. Mech.*, vol. 1, pp. 288–293, 2011.
19. M. A. EL-AZIZ and A. S. YAHYA, "Heat and mass transfer of unsteady hydromagnetic free convection flow through porous medium past a vertical plate with uniform surface heat flux," *J. Theor. Appl. Mech. Sofia*, vol. 47, no. 3, pp. 25–58, 2017.
20. M. K. Nayak, G. C. Dash, and L. P. Singh, "Heat and mass transfer effects on MHD viscoelastic fluid over a stretching sheet through porous medium in presence of chemical reaction," *Propuls. Power Res.*, vol. 5, no. 1, pp. 70–80, 2016.
21. Swain, S. R. Mishra, and H. B. Pattanayak, "Flow over Exponentially Stretching Sheet through Porous Medium with Heat Source/Sink," *Hindawi Publ. Corp. J. Eng.*, 2015.
22. S. U. S. Choi, "Enhancing thermal conductivity of fluids with nanoparticle in the development of and application of non-Newtonian flow," *ASME FED*, vol. 66, pp. 99–105, 1995.
23. A. Ebaid, F. Al Mutairi, and S. M. Khaled, "Effect of Velocity Slip Boundary Condition on the Flow and Heat Transfer of Cu-Water and TiO2-Water Nanofluids in the Presence of a Magnetic Field," *Adv. Math. Phys.*, 2014.
24. W. Ibrahim, "Magnetohydrodynamic(MHD) boundary layer stagnation point flow and heat transfer of a nanofluid past a stretching sheet with melting," *Propuls. Power Res.*, vol. 6, no. 3, pp. 214–222, 2017.
25. P. B. A. Reddy, S. Suneetha, and N. B. Reddy, "Numerical study of magnetohydrodynamics (MHD) boundary layer slip flow of a Maxwell nanofluid over an exponentially stretching surface with convective boundary condition," *Propuls. Power Res.*, vol. 6, no. 4, pp. 259–268, 2017.
26. Y. S. Daniel, Z. A. AziZ, U. Ismail, and F. Salah, "Thermal stratification effects on MHD radiative flow of nanofluid over nonlinear stretching sheet with variable thickness," *J. Comput. Des. Eng.*, vol. 5, pp. 232–242, 2018.
27. S. R. C, K. Naikotib, and M. R. Mehdi, "MHD flow and heat transfer characteristics of Williamson nanofluid over a stretching sheet with variable thickness and variable thermal conductivity," *Trans. A. Razmadze Math. Inst.*, vol. 171, pp. 195–211, 2017.
28. A. A. Ahmed, "Effects of thermal diffusion and diffusion thermo on free convective heat and mass transfer over a

stretching surface considering suction or injection," *Commun. Nonlinear Sci. Numer. Simul*, vol. 14, pp. 2202–2214, 2009.
29. H. C. Brinkman, "The viscosity of concentrated suspensions and solution," *J. Chem. Phys*, vol. 20, pp. 571–581, 1952.
30. J. C. M. Garnett, "Colors in metal glasses and in metallic films," *Philos. Trans. R. Soc. Lond.*, vol. A203, pp. 385–420, 1904.
31. C.-A. Guérin, P. Mallet, and A. Sentenac, "Effective-medium theory for finite-size aggregates," *J. Opt. Soc. Am*, vol. A23, no. 2, pp. 349–358, 2006.
32. G. Bal Reddy., B. Shankar Goud., and MN. Raja Shekar., "Implicit finite difference solution of radiation effects on MHD fluid flow of a nanofluid past an exponential stretching sheet embedded in a porous medium", *Journal of Advance Research in Dynamical & Control Systems*, Vol. 10, 06-Special Issue, 2018. pp.746-760.
33. M. M.Nandeppanavar, K.Vajravelu, and P.S.Datti, "Optimal homotopy asymptotic solutions for nonlinear ordinary differential equations arising in flow and heat transfer due to non-linear stretching sheet," *Heat-trans. Asian Res.*, vol. 45, no. 1, pp. 15–29, 2016.
34. Y. Yirga and D. Tesfay, "Heat and Mass Transfer in MHD Flow of Nanofluids through a Porous Media Due to a Permeable Stretching Sheet with Viscous Dissipation and Chemical Reaction Effects," *World Acad. Sci. Eng. Technol. Int. J. Mech. Mechatronics Eng.*, vol. 9, pp. 709–716, 2015.
35. M. . Hamad, "Analytical solution of natural convection flow of a nanofluid over a linearly stretching sheet in the presence of magnetic field," *Int. Commun. Heat Masstrans.*, vol. 38, no. 4, pp. 487–492, 2011.
36. H. F. Oztop and E. Abu-Nada, "Numerical study of natural convection in partially heated rectangular enclosures filled with nanofluids," *Int. J. Heat Fluid Flow*, vol. 29, pp. 1326–1336, 2008.